IC/90/385

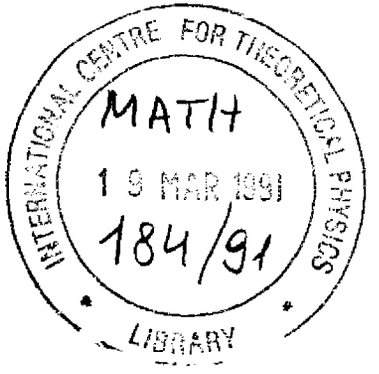

INTERNATIONAL CENTRE FOR THEORETICAL PHYSICS

ON TESTS OF RANDOMNESS FOR SPATIAL POINT PATTERNS

Sani I. Doguwa

INTERNATIONAL ATOMIC ENERGY AGENCY

UNITED NATIONS EDUCATIONAL, SCIENTIFIC AND CULTURAL ORGANIZATION

1990 MIRAMARE - TRIESTE

IC/90/385

International Atomic Energy Agency

and

United Nations Educational Scientific and Cultural Organization

INTERNATIONAL CENTRE FOR THEORETICAL PHYSICS

ON TESTS OF RANDOMNESS FOR SPATIAL POINT PATTERNS *

Sani I. Doguwa **

International Centre for Theoretical Physics, Trieste, Italy.

ABSTRACT

New tests of randomness for spatial point patterns are introduced. These test statistics are then compared in a power study with the existing alternatives. These results of the power study suggest that one of the tests proposed is extremely powerful against both aggregated and regular alternatives.

MIRAMARE – TRIESTE

November 1990

* Submitted for publication.

** Permanent address: Department of Mathematics, Ahmadu Bello University, Zaria, Nigeria.

1 Introduction

System of points like trees in a forest, plants in a field or towns in a region can be described by their locations in two dimensional space. These descriptions are examples of spatial point patterns in two dimensions. We assume that the observed mapped spatial point pattern is a realization of a spatial point process model which is stationary and isotropic. Obviously a question arises such as "Can the towns be considered as randomly distributed over a given region ?" This paper is concerned with testing whether a spatial point pattern is consistent with the null hypothesis of randomness.

There are some important functions which characterize distributional properties of spatial point processes. Such functions include the second order function K(t), the product density $\rho^{(2)}(t)$, and the pair correlation function g(t). The function defined through the relation,

$$\lambda K(t) = E[N_o(t)] \tag{1}$$

where $N_o(t)$ is the number of other points within distance t of an arbitrary point, is called the K(t) function. The parameter λ is the mean number of points per unit area.

The function $\rho^{(2)}(t)$, is defined by

$$\rho^{(2)}(t) = \frac{\lambda^2}{2\pi t}\frac{dK(t)}{dt} \tag{2}$$

The value of $\rho^{(2)}(t)$ can be interpreted as the joint density for the occurrence of two points of the process that are a distance t apart. The g(t) function is connected with the $\rho^{(2)}(t)$ function through the relation

$$g(t) = \frac{\rho^{(2)}(t)}{\lambda^2} \tag{3}$$

RIPLEY(1977) proposed an edge-corrected estimate of K(t) as

$$\hat{K}(t) = \frac{A}{n(n-1)}\sum_{i=1}^{n}\sum_{j\neq i}^{n} I_{ij}S_{ij} \tag{4}$$

where $I_{ij} = 0$ if the distance r_{ij} between the i^{th} point and the j^{th} point in the window W is more than t, and $I_{ij} = 1$, otherwise. The constant A is the area of W and n is the number of points in it. The value S_{ij} defined by

$$S_{ij} = \frac{2\pi r_{ij}}{v|W \cap \delta b(x_i, r_{ij})|} \tag{5}$$

takes care of the edge effects in W. Here $v|W \cap \delta b(z, f)|$ is a one dimensional Lebesque measure on $\delta b(z, f)$, the boundary of the circle b(z,f), with centre z and radius f. Various estimators of K(t) have been proposed by, for example, OHSER and STOYAN(1981) and DOGUWA and UPTON(1989).

Two test statistics associated with (4) are the r and L_m statistics defined by

$$r = Sup_{t \le t_o}\{|\ \hat{K(t)} - \pi t^2\ |\} \tag{6}$$

and

$$L_m = Sup_{t \le t_o}\{|\ \sqrt{\hat{K(t)}/\pi} - t\ |\} \tag{7}$$

respectively. The upper limit t_o was set at $1.25/\sqrt{\lambda}$.

FIKSEL(1988) and DOGUWA(1990) proposed various estimators of the g(t) function. The results in DOGUWA(1990) suggest using the estimator $\hat{g(t)}$ defined by

$$\hat{g(t)} = \frac{A}{n(n-1)} \sum_{i=1}^{n} \sum_{j \ne i}^{n} \gamma_{ij}(t) S_{ij} \tag{8}$$

to estimate g(t). Here $\gamma_{ij}(t)$ is given by

$$\gamma_{ij}(t) = \frac{1}{2\pi h r_{ij}} \{k(\frac{r_{ij} - t}{h}) + k(\frac{r_{ij} + t}{h})\} \tag{9}$$

where k(y) is the kernel and h is the band-width parameter. A suitable kernel k(y) is the EPANECHNIKOV(1969) kernel, which is defined by

$$k(y) = \begin{cases} \frac{3}{4\sqrt{5}}(1 - \frac{y^2}{5}) & \text{if } |\ y\ | \le \sqrt{5} \\ 0 & \text{otherwise} \end{cases}$$

From computational and simulation studies FIKSEL(1988) suggests that a choice of h as

$$h = 0.1/\sqrt{\lambda}$$

is appropriate in two dimensions. A natural statistic for test of randomness using (8) is

$$\gamma = Sup_{t \le t_o}\{|\ \hat{g(t)} - 1\ |\} \tag{10}$$

This paper proposes new test statistics based on the characteristic variants of (4) and (8). These tests statistics are then compared using Monte Carlo tests for cases of aggregated and regular alternatives. Furhtermore, the true values of these characteristics are determined under the null hypothesis of randomness, using simulation methods. As an example of the use of these characteristics, the nesting pattern of eastern Willets (*Catoptrophorus Semipalmatus*) is analysed.

2 Characteristic variants of $\hat{K(t)}$

DOGUWA(1989) provides three characteristic variants of $\hat{K(t)}$, namely $\hat{U_k(t)}$, $\hat{V_k(t)}$, and $\hat{R_k(t)}$, which are defined by

$$\hat{R_k(t)} = Max_{1 \le i \le n}\{\sqrt{\hat{K_i(t)}/\pi}\} \tag{11}$$

$$\hat{U_k(t)} = \frac{1}{n} \sum_{i=1}^{n} \sqrt{\hat{K_i(t)}/\pi} \tag{12}$$

$$\hat{V_k(t)} = \frac{1}{n} \sum_{i=1}^{n} \{\hat{K_i(t)}/\pi\}^2 \tag{13}$$

where $\hat{K_i(t)}$ is the estimate of the second order neighbourhood function $K_i(t)$ of GETIS and FRANKLIN(1987). This estimate is given by

$$\hat{K_i(t)} = \frac{A}{n-1} \sum_{j \ne i}^{n} I_{ij} S_{ij} \tag{14}$$

For a Poisson process, we expect the true values of the characteristics (11) to (13) to be t, t and t^4 respectively. In practice, however, the true values of (11) and (13) are significantly different from t and t^4 respectively. The true values of (12) and (13) are determined under the null hypothesis of randomness by simulation methods. We assume that these characteristics are not significantly affected by the boundary of W, because of the inherent edge correction in the estimate $\hat{K_i(t)}$.

In our effort to determine the true values of these characteristics we used a unit square window. We used values of n between 15 and 90 points and for each n we used 1000 realizations of the Poisson process in the unit square. After examination of a large number of scattergrams we arrived at the following approximated values

$$V_k(t) = 2.086 t^{2.8 - 0.001\lambda} / \lambda^{0.698} \tag{15}$$

and

$$R_k(t) = 3.6t^{2\lambda^{-0.288}}/\lambda^{0.32} \tag{16}$$

Using both a unit square window and a rectangular window of sides $10\sqrt{0.1}$ by $\sqrt{0.1}$ we computed the bias of $V_k\hat{(t)}$ and $R_k\hat{(t)}$ for a Poisson process of intensity $\lambda = 25$ and $\lambda = 100$ respectively. The bias of $R_k\hat{(t)}$ is plotted against t in Fig.1. These plots suggest that $E\{R_k\hat{(t)}\} \gg t$. However (16) seems to be a good approximation of the true value of $R_k(t)$, under the null hypothesis of randomness. Similar results are obtained for other values of λ.

The values for the bias of $V_k\hat{(t)}$ are plotted against t in Fig.2. The bias plot suggests that $E\{V_k\hat{(t)}\} \gg t^4$. It is clear from this plot that (15) gives a much smaller bias for small distances. This therefore suggests that (15) approximates well the true value of $V_k(t)$ for a Poisson process. Similar results are obtained for other values of λ.

The three characteristic variants of $K\hat{(t)}$ provide three test statistics for test of spatial randomness. These are:

$$f_k = Sup_{t \le t_o}\{|\ R_k\hat{(t)} - R_k(t)\ |\} \tag{17}$$

$$g_k = Sup_{t \le t_o}\{|\ U_k\hat{(t)} - t\ |\} \tag{18}$$

$$d_k = Sup_{t \le t_o}\{|\ V_k\hat{(t)} - V_k(t)\ |\} \tag{19}$$

Note that these three statistics were suggested by DOGUWA(1989), but with $R_k(t)$ and $V_k(t)$ replaced by t and t^4 respectively.

3 Characteristic variants of $g\hat{(t)}$

Closely related to the second-order neighbourhood function $K_i(t)$, is the function $\rho^{(2)}(i,t)$, defined by

$$\rho^{(2)}(i,t) = \frac{\lambda^2}{2\pi t}\frac{dK_i(t)}{dt} \tag{20}$$

The value of $\rho^{(2)}(i,t)$ can be interpreted as the joint density for the occurence of a pair of points that are a distance t apart and having as one of

its members a given point i. Another function g(i,t) is also related to the $K_i(t)$ function through the relation

$$g(i,t) = \frac{\rho^{(2)}(i,t)}{\lambda^2}$$

An edge-corrected estimator of $g(i,t)$ for positive values of t is given by

$$g\hat{(i,t)} = \frac{A}{n-1}\sum_{j \ne i}^{n}\gamma_{ij}(t)S_{ij} \tag{21}$$

where S_{ij} and $\gamma_{ij}(t)$ are as defined in (5) and (9), respectively. Also n and A are as defined in (4).

The estimate of g(i,t) is used to provide the characteristic variants of $g\hat{(t)}$ as

$$R_\rho\hat{(t)} = Max_{1 \le i \le n}\{\sqrt{g\hat{(i,t)}}\} \tag{22}$$

$$U_\rho\hat{(t)} = \frac{1}{n}\sum_{i=1}^{n}\sqrt{g\hat{(i,t)}} \tag{23}$$

and

$$V_\rho\hat{(t)} = \frac{1}{n}\sum_{i=1}^{n}\{g\hat{(i,t)}\}^2 \tag{24}$$

We expect the true values of $R_\rho(t)$, $U_\rho(t)$, and $V_\rho(t)$ to be close to 1. In practice, this is not the case. For reasons of tractability we used simulations to obtain good approximation to the true values of these characteristics for a Poisson process in terms of t and the intensity λ.

We used values of n between 15 and 90 in the unit square. For each n we simulated 1000 realizations of the Poisson process and computed the three variants for various values of t. After examination of a large number of scattergrams we arrived at the following approximations,

$$R_\rho(t) = 2.292/\lambda^{0.168}t^{0.022\lambda^{0.553}} \tag{25}$$

$$U_\rho(t) = 0.783\lambda^{0.145}t^{0.24} \tag{26}$$

$$V_\rho(t) = 3.305/\lambda^{0.84}t^{0.455\lambda^{0.121}} \tag{27}$$

We then computed the bias of (22), (23) and (24) for a Poisson process in the unit square with intensities $\lambda = 25$, and $\lambda = 90$ respectively. Fig.3 presents a plot of the bias of $R_\rho\hat{(t)}$ against t. It is clear from this Figure

that $E\{\hat{R_\rho}(t)\} \gg 1$ for all values of t considered. However, equation (25) seems to be a good approximation to the true value of $R_\rho(t)$.

Figures (4 and 5) present the plots of the bias of $\hat{U_\rho}(t)$ and $\hat{V_\rho}(t)$ respectively against t. It is clear from these figures that $E\{\hat{U_\rho}(t)\} \ll 1$, whereas $E\{\hat{V_\rho}(t)\} \gg 1$, for the values of t considered. These suggest that (26) and (27) are good approximations to the true values of $U_\rho(t)$ and $V_\rho(t)$ for a Poisson process.

The characteristics $\hat{R_\rho}(t)$, $\hat{U_\rho}(t)$ and $\hat{V_\rho}(t)$ provide the new statistics for testing the null hypothesis of randomness. These test statistics are given by

$$f_\rho = Sup_{t \le t_o}\{\mid \hat{R_\rho}(t) - R_\rho(t) \mid\} \tag{28}$$

$$g_\rho = Sup_{t \le t_o}\{\mid \hat{U_\rho}(t) - U_\rho(t) \mid\} \tag{29}$$

$$d_\rho = Sup_{t \le t_o}\{\mid \hat{V_\rho}(t) - V_\rho(t) \mid\} \tag{30}$$

4 Power study

We compare the power of the new statistics with the range of alternatives discussed previously in Sections 1 and 2. The simulations involve patterns of $n = 25$ and $n = 90$ points in the unit square. All the statistics were computed for values of $t = \beta t_o/100$, where $\beta = 1, 2, \ldots, 100$.

The alternative processes considered were the Poisson cluster processes with parameters μ and σ; and the Strauss processes with parameters r and c. The Poisson cluster process gives a highly clustered pattern whenever μ is large and $\sigma \to 0$. Similarly the Strauss process, simulated by the algorithm of RIPLEY(1979) gives a hardcore process with interaction range r whenever $c = 0$.

The test statistics were implemented by the straightforward Monte Carlo approach and the Monte Carlo 4% significant points were derived using 999 and 199 simulations repectively for small and moderately large samples of the Poisson process in the unit square.

Fifty realizations were generated for each process and a range of parameter values. Tables 1 and 2 record the numbers of occasions on which the hypothesis of a Poisson process was rejected by a 4% test based on each of the statistics discussed previously.

For small samples, it is clear that the statistics L_m, r and g_ρ are the most powerful against clustered alternatives, whereas g_k is the most powerful against regularity. However, the statistic L_m seems to be more robust for small samples in that it is powerful against both alternatives.

For the case of moderately large samples, the statistic r is the most powerful against aggregated patterns, followed very closely by g_ρ and L_m; whereas g_k, L_m and g_ρ are the most powerful against regularity. For highly and moderately clustered and regular patterns, the statistic g_ρ is more robust than the other statistics considered.

In conclusion, the statistics r, L_m and g_ρ are powerful detectors of clustered patterns while g_ρ, g_k and L_m are powerful against regularity.

5 Analysis of Willets nest pattern

Willets nest in two disjunct populations in North America. HOWE(1982) described on the basis of observations of marked adults, the spatial structure of the breeding Willets population. Fig 6a presents a detailed map of the study area which was prepared from low altitude infrared aerial photographs. DOGUWA(1989) explored this nesting pattern using the g(t) function. His results suggest some possible evidence of nest spacing for values of t less than 20 metres.

Our objective is to analyse this pattern using the statistics considered in the previous section, for any deviation from the null hypothesis of randomness. Table 3a gives the observed values of the statistics r, L_m, g_k and g_ρ for the nest pattern together with the corresponding 1% critical values obtained from 99 realizations of the Poisson process with the same point intensity and in the same size window as the nest pattern.

All the observed values for these test statistics are not significant at the 1% level. Fig 6b presents the plots of

$$G_\rho(t) = \hat{U_\rho}(t) - U_\rho(t)$$

against t, together with the lower and upper 99% simulation envelopes. The values of $G_\rho(t)$ for the observed nest pattern lie entirely within the acceptance region, suggesting that the willets nesting pattern is consistent with the hypothesis of a Poisson process.

6 Conclusion

Various tests of randomness for spatial point patterns based on inter-point distances are considered in this paper. We shall conclude by noting that the rejection of the null hypothesis of a Poisson process by any of the test statistics considered in the previous section, implies that the observed pattern under investigation is not random. However a pattern that is clearly non-random can still be accepted as random by these test statistics. Furthermore,the rejection of the null hypothesis by any of the statistics considered cannot tell us much about the nature of the interaction of the points in the pattern.

A plot of the associated characteristics against t may give us the required information. As an example, consider a realization of a Strauss process with $c = 0$ and $r = 0.07$ in the unit square. This realization is illustrated in Fig 7a. The observed values of the statistics r,L_m, g_ρ and g_k for this realization, together with the 1% critical points are presented in Table 3b. The statistics L_m and g_k were able to detect the small scale regularity in the data. However the statistics r and g_ρ were not able to detect the apparent regularity in the pattern.

On examination of the plots of $G_\rho(t)$ against t for this pattern, together with the 99% confidence envelopes, it is clear that the values of $G_\rho(t)$ for the data in Fig 7a penetrates the lower envelope for values of t in the region of 0.05 units. This suggests a significant departure from the randomness hypothesis towards a regular alternative.

Acknowledgements

The author would like to thank Professor Abdus Salam, the International Atomic Energy Agency and UNESCO for hospitality at the International Centre for Theoretical Physics, Trieste Italy. He is also grateful to Ahmadu Bello University Zaria - Nigeria for allowing him to visit I.C.T.P as a Visiting Scientist.

References

[1] DOGUWA, S.I.(1989). On Second Order Neighbourhood Analysis of Mapped Point Patterns. **Biom. J. 31**, 451- 459.

[2] DOGUWA, S.I.(1990). On edge-corrected kernel-based pair correlation function estimators for point processes.**Biom. J. 32**, 95-106.

[3] DOGUWA, S.I. and UPTON, G.J.G.(1989). Edge-corrected estimators for the reduced second moment measure of point processes. **Biom.J. 31**, 563-575.

[4] EPANECHNIKOV, V.A.(1969). Non-parametric Estimation of a Multidimensional Probability Density.**Theor. Probabs. Appl.** 14, 153-158

[5] FIKSEL, T.(1988). Edge-corrected Density Estimators for Point Processes. **Statistics. 19**, 67-75.

[6] GETIS, A. and FRANKLIN, J.(1987). Second Order Neighbourhood Analysis of Mapped Point Patterns. **Ecology.** 68, 473-477.

[7] OHSER, J. and STOYAN, D.(1981). On the second-order and orientation analysis of planar stationary point processes. **Biom. J. 23**, 523-533.

[8] RIPLEY, B.D.(1977). Modelling Spatial Patterns (with discussion). **J. Roy. Statist. Soc. B39**, 172 - 212.

[9] RIPLEY, B.D.(1979). Simulating Spatial Patterns: Dependent Samples from a Multivariate Density. **Appl. Statist. 28**, 109-112.

Table 1: Numbers of occasions in which a test of randomness at the 4% level resulted in rejection of the null hypothesis when the data arose from a Poisson cluster process (parents retained) with parameters μ and σ

		$\begin{pmatrix} r & f_k & f_\rho \\ L_m & g_k & g_\rho \\ \gamma & d_k & d_\rho \end{pmatrix}$		
		$n = 25$		
σ =	0.04	0.08	0.12	
$\mu = 1$	$\begin{pmatrix} 36 & 39 & 11 \\ 50 & 38 & 50 \\ 37 & 27 & 12 \end{pmatrix}$	$\begin{pmatrix} 23 & 16 & 7 \\ 28 & 6 & 38 \\ 8 & 19 & 7 \end{pmatrix}$	$\begin{pmatrix} 24 & 8 & 6 \\ 15 & 2 & 14 \\ 6 & 17 & 6 \end{pmatrix}$	
$\mu = 2$	$\begin{pmatrix} 50 & 48 & 50 \\ 50 & 50 & 50 \\ 50 & 32 & 36 \end{pmatrix}$	$\begin{pmatrix} 45 & 32 & 13 \\ 48 & 29 & 50 \\ 26 & 32 & 17 \end{pmatrix}$	$\begin{pmatrix} 36 & 19 & 8 \\ 32 & 14 & 35 \\ 18 & 31 & 11 \end{pmatrix}$	
$\mu = 3$	$\begin{pmatrix} 50 & 50 & 39 \\ 50 & 50 & 50 \\ 50 & 38 & 44 \end{pmatrix}$	$\begin{pmatrix} 50 & 43 & 22 \\ 50 & 49 & 50 \\ 38 & 39 & 27 \end{pmatrix}$	$\begin{pmatrix} 45 & 16 & 16 \\ 40 & 16 & 43 \\ 25 & 40 & 17 \end{pmatrix}$	
		$n = 90$		
$\mu = 1$	$\begin{pmatrix} 50 & 21 & 6 \\ 50 & 21 & 50 \\ 33 & 40 & 10 \end{pmatrix}$	$\begin{pmatrix} 44 & 5 & 4 \\ 44 & 0 & 44 \\ 8 & 38 & 4 \end{pmatrix}$	$\begin{pmatrix} 38 & 3 & 2 \\ 32 & 0 & 8 \\ 2 & 32 & 2 \end{pmatrix}$	
$\mu = 2$	$\begin{pmatrix} 50 & 41 & 24 \\ 50 & 50 & 50 \\ 50 & 47 & 28 \end{pmatrix}$	$\begin{pmatrix} 50 & 13 & 14 \\ 50 & 14 & 50 \\ 24 & 48 & 14 \end{pmatrix}$	$\begin{pmatrix} 48 & 5 & 48 \\ 36 & 4 & 31 \\ 13 & 40 & 12 \end{pmatrix}$	
$\mu = 3$	$\begin{pmatrix} 50 & 47 & 36 \\ 50 & 50 & 50 \\ 50 & 50 & 43 \end{pmatrix}$	$\begin{pmatrix} 50 & 27 & 26 \\ 50 & 36 & 50 \\ 42 & 50 & 28 \end{pmatrix}$	$\begin{pmatrix} 48 & 16 & 12 \\ 46 & 5 & 44 \\ 28 & 46 & 18 \end{pmatrix}$	

Table 2: Numbers of occasions in which a test of randomness at the 4% level resulted in rejection of the null hypothesis when the data arose from a Strauss process with interaction range r and strength c.

		$\begin{pmatrix} r & f_k & f_\rho \\ L_m & g_k & g_\rho \\ \gamma & d_k & d_\rho \end{pmatrix}$		
		$n = 25$		
c =	0.0	0.15	0.3	
$r = 0.10$	$\begin{pmatrix} 0 & 50 & 0 \\ 50 & 50 & 0 \\ 0 & 0 & 0 \end{pmatrix}$	$\begin{pmatrix} 1 & 7 & 0 \\ 29 & 42 & 0 \\ 0 & 0 & 0 \end{pmatrix}$	$\begin{pmatrix} 0 & 1 & 0 \\ 11 & 18 & 0 \\ 0 & 0 & 0 \end{pmatrix}$	
$r = 0.125$	$\begin{pmatrix} 0 & 50 & 0 \\ 50 & 50 & 0 \\ 0 & 0 & 0 \end{pmatrix}$	$\begin{pmatrix} 0 & 3 & 0 \\ 30 & 44 & 0 \\ 0 & 0 & 0 \end{pmatrix}$	$\begin{pmatrix} 1 & 27 & 0 \\ 11 & 27 & 0 \\ 0 & 0 & 0 \end{pmatrix}$	
$r = 0.150$	$\begin{pmatrix} 50 & 49 & 0 \\ 50 & 50 & 50 \\ 0 & 0 & 0 \end{pmatrix}$	$\begin{pmatrix} 1 & 3 & 0 \\ 35 & 49 & 0 \\ 0 & 0 & 0 \end{pmatrix}$	$\begin{pmatrix} 0 & 0 & 1 \\ 13 & 32 & 1 \\ 1 & 0 & 1 \end{pmatrix}$	
		$n = 90$		
$r = 0.025$	$\begin{pmatrix} 0 & 50 & 48 \\ 48 & 21 & 48 \\ 0 & 0 & 0 \end{pmatrix}$	$\begin{pmatrix} 0 & 28 & 26 \\ 35 & 15 & 36 \\ 0 & 0 & 0 \end{pmatrix}$	$\begin{pmatrix} 2 & 16 & 15 \\ 22 & 11 & 21 \\ 2 & 0 & 2 \end{pmatrix}$	
$r = 0.045$	$\begin{pmatrix} 4 & 50 & 50 \\ 50 & 50 & 50 \\ 0 & 0 & 0 \end{pmatrix}$	$\begin{pmatrix} 2 & 21 & 17 \\ 50 & 50 & 50 \\ 0 & 0 & 0 \end{pmatrix}$	$\begin{pmatrix} 0 & 16 & 9 \\ 41 & 50 & 37 \\ 0 & 0 & 0 \end{pmatrix}$	
$r = 0.065$	$\begin{pmatrix} 50 & 50 & 50 \\ 50 & 50 & 50 \\ 0 & 3 & 0 \end{pmatrix}$	$\begin{pmatrix} 32 & 29 & 19 \\ 50 & 50 & 50 \\ 0 & 0 & 0 \end{pmatrix}$	$\begin{pmatrix} 22 & 18 & 9 \\ 48 & 50 & 43 \\ 0 & 0 & 2 \end{pmatrix}$	

Table 3a: The observed values of the statistics r, L_m, g_k and g_ρ for the Willets nest pattern of Fig 6a, together with the 1% critical values obtained from 99 realizations of the Poisson process with 35 points in the region 750m by 167.5m

Test statistic	Observed value	1% Critical point
r	4380.0	5899.62
L_m	9.0345	17.2224
g_k	16.074	22.902
g_ρ	0.49204	0.88058

Table 3b: The observed values of the test statistics r, L_m, g_k and g_ρ for the Strauss process of Fig 7a, together with the 1% critical values obtained from 99 realizations of the Poisson process with 35 points in the unit square.

Test statistic	Observed value	1% Critical point
r	0.026989	0.048212
L_m	0.0718388*	0.045474
g_k	0.075570*	0.069827
g_ρ	0.58158	0.75866

FIGURE CAPTIONS

Fig 1: The plots of the bias: $E\{\hat{R_k(t)}\} - R_k(t)$ [-□-] and $E\{R_k(t)\} - t$ [-×-] for a Poisson process of intensity $\lambda = 100$ in (a) unit square and (b) rectangle

Fig 2: The plots of the bias: $E\{\hat{V_k(t)}\} - V_k(t)$ [-□-] and $E\{\hat{V_k(t)}\} - t^4$ [-×-] for a Poisson process of intensity $\lambda = 25$ in (a) unit square and (b) rectangle.

Fig 3: The plots of the bias: $E\{\hat{R_\rho(t)}\} - R_\rho(t)$ [-○-] and $E\{\hat{R_\rho(t)}\} - 1$ [-△-] for a Poisson process of intensity (a) $\lambda = 25$ and (b) $\lambda = 90$ in a unit square.

Fig 4: The plots of the bias: $E\{\hat{U_\rho(t)}\} - U_\rho(t)$ [-○-] and $E\{\hat{U_\rho(t)}\} - 1$ [-△-] for a Poisson process of intensity (a) $\lambda = 25$ and (b) $\lambda = 90$ in a unit square.

Fig 5: The plots of the bias: $E\{\hat{V_\rho(t)}\} - V_\rho(t)$ [-□-] and $E\{\hat{V_\rho(t)} - 1$ [-△-] for a Poisson process of intensity (a) $\lambda = 25$ and (b) $\lambda = 90$ in a unit square.

Fig 6: (a) Positions of the Willets nest in a 750m by 167.5m region. (b) A plot of $G_\rho(t)$ [-○-] for the nest pattern. The solid lines are the envelopes estimated from 99 simulations of a Poisson process with $n = 35$ points in the same size window as the nest pattern.

Fig 7: (a) Example realization of a Strauss process with $c = 0, r = 0.07$ in a unit square. (b) A plot of $G_\rho(t)$ [-○-] for the data in (a). The solid lines are the envelopes estimated from 99 realizations of a Poisson process with $n = 35$ points in a unit square.

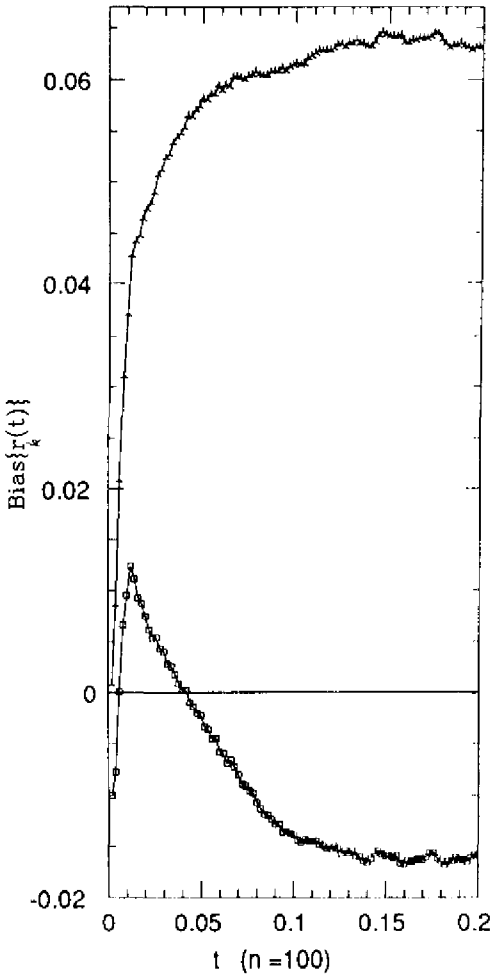

Fig.1a

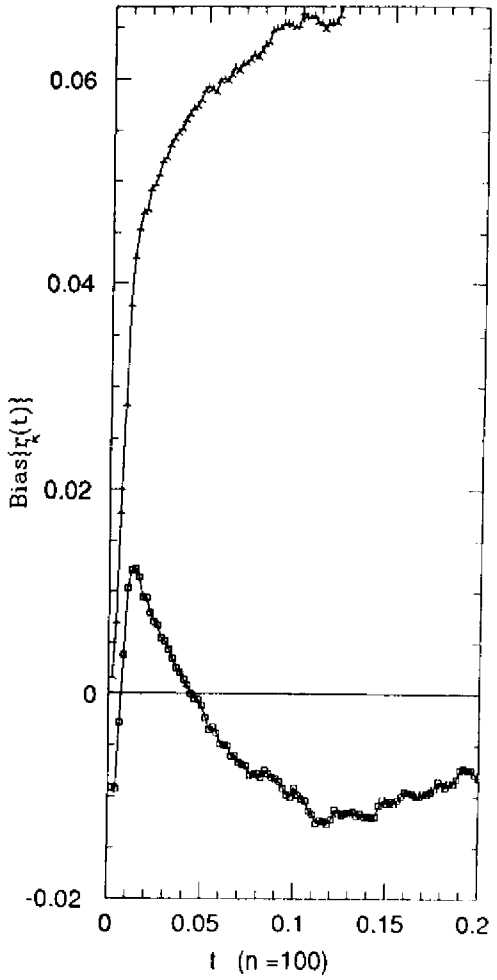

Fig.1b

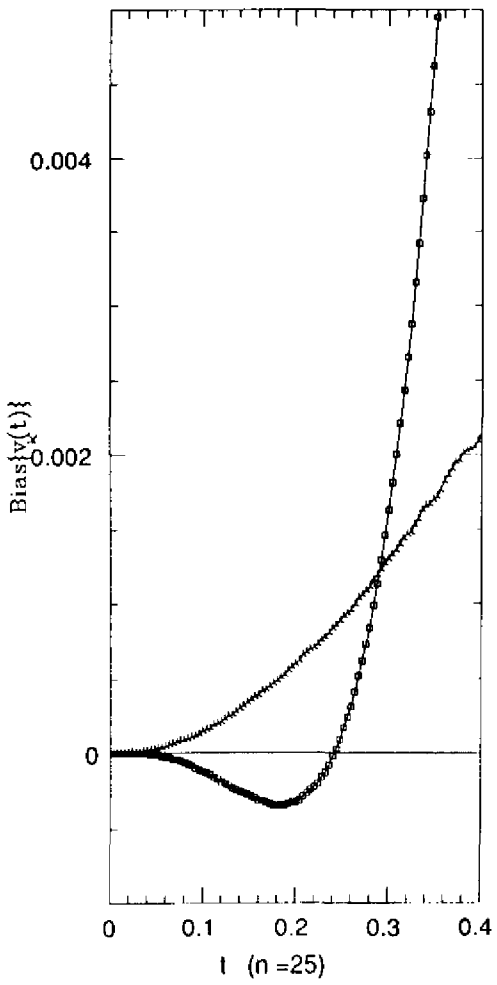

Fig.2a

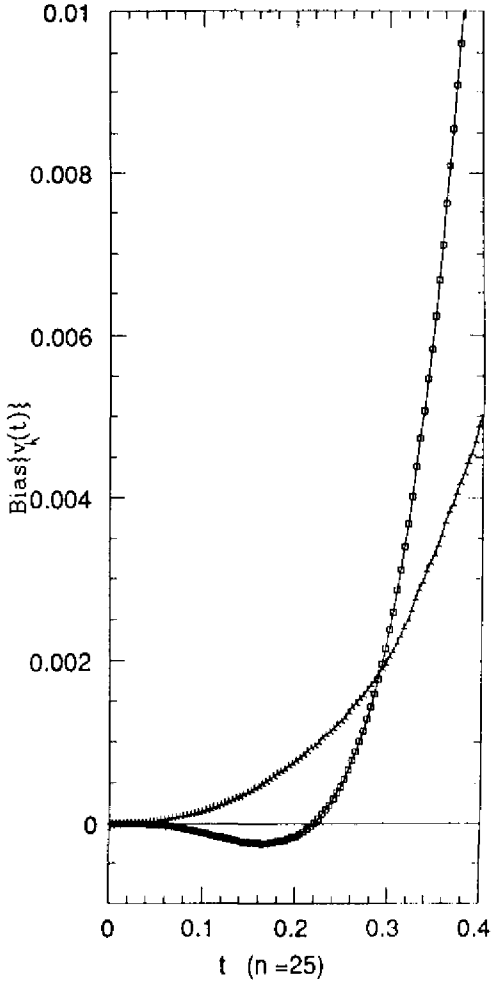

Fig.2b

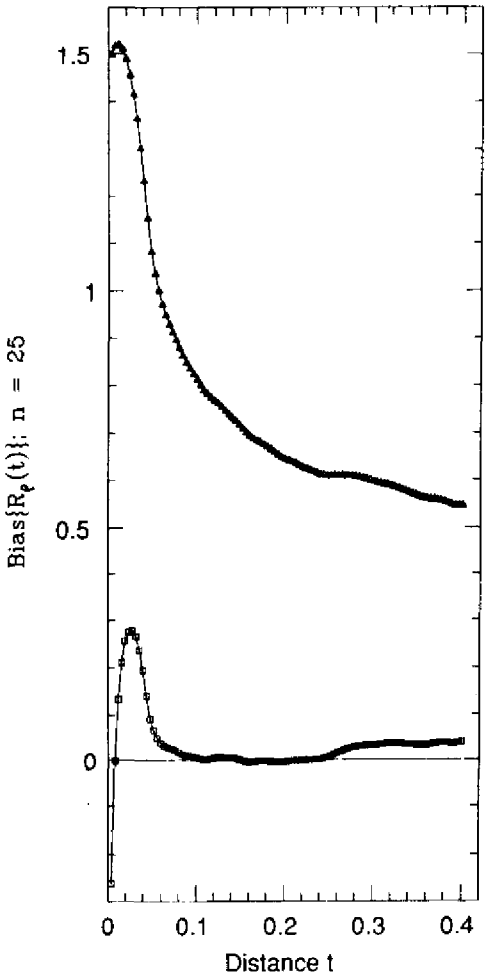

Fig.3a

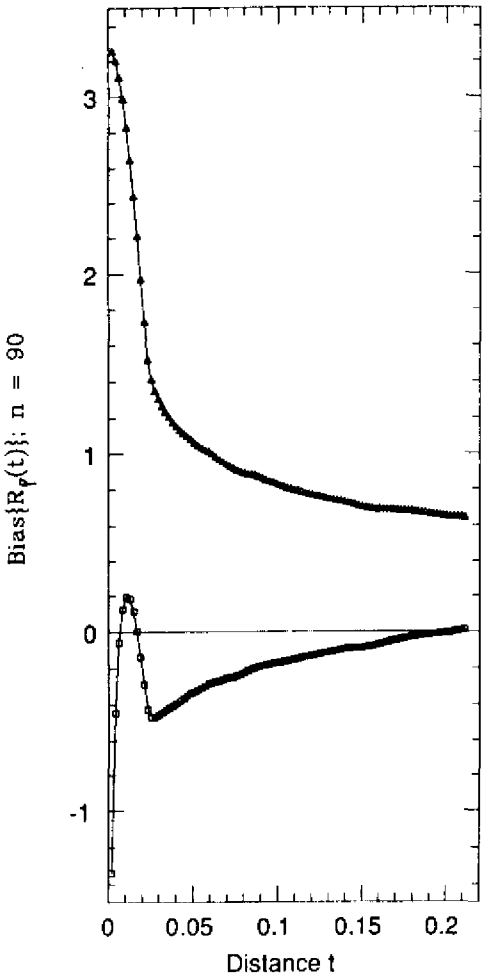

Fig.3b

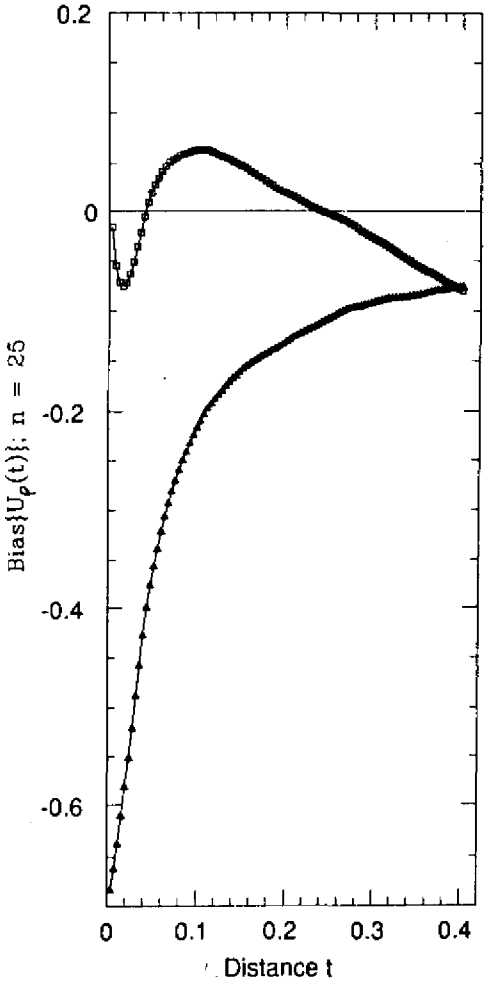

Fig.4a

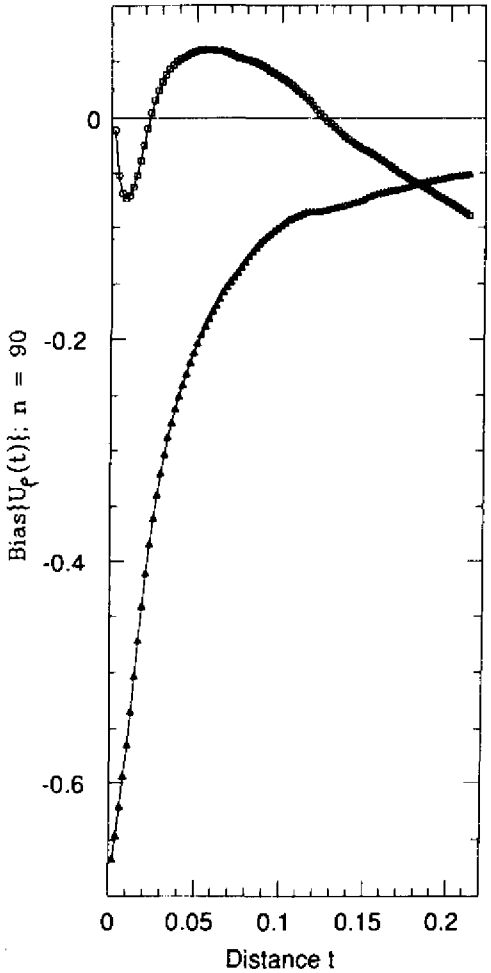

Fig.4b

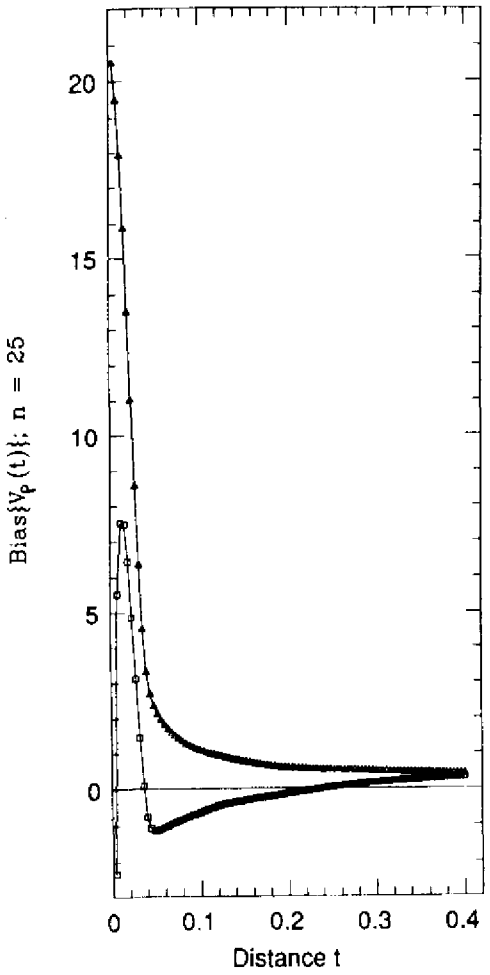

Fig.5a

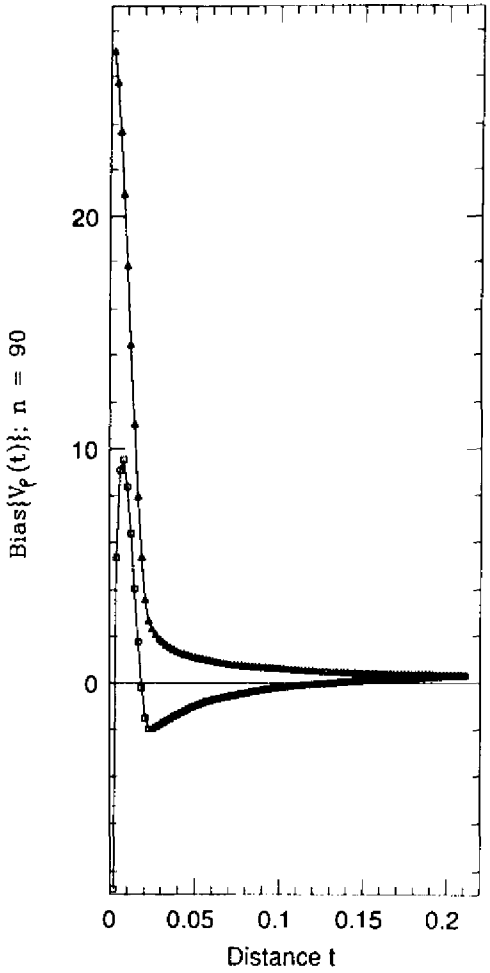

Fig.5b

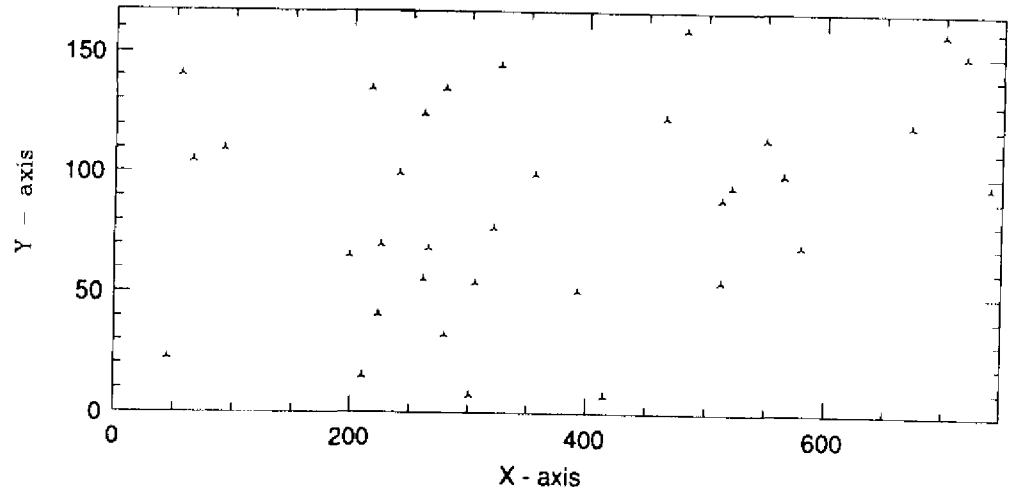

Fig.6a

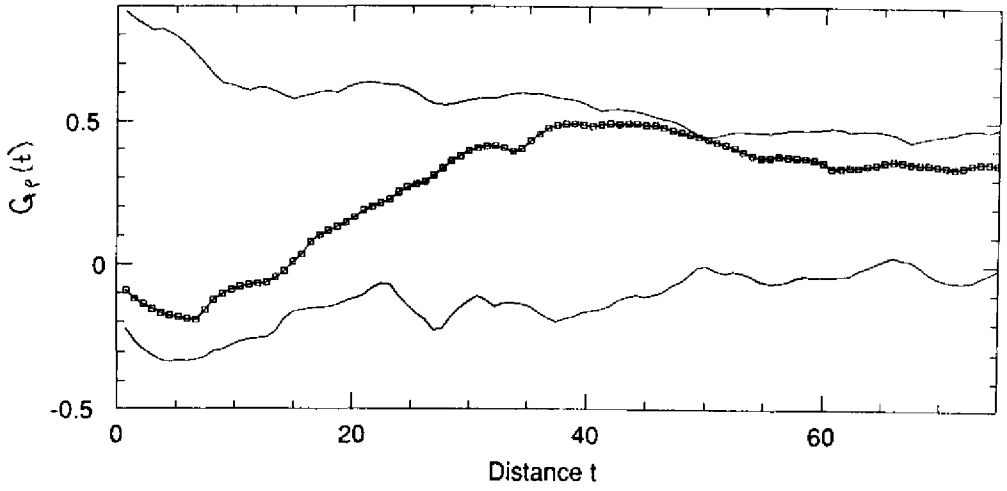

Fig.6b

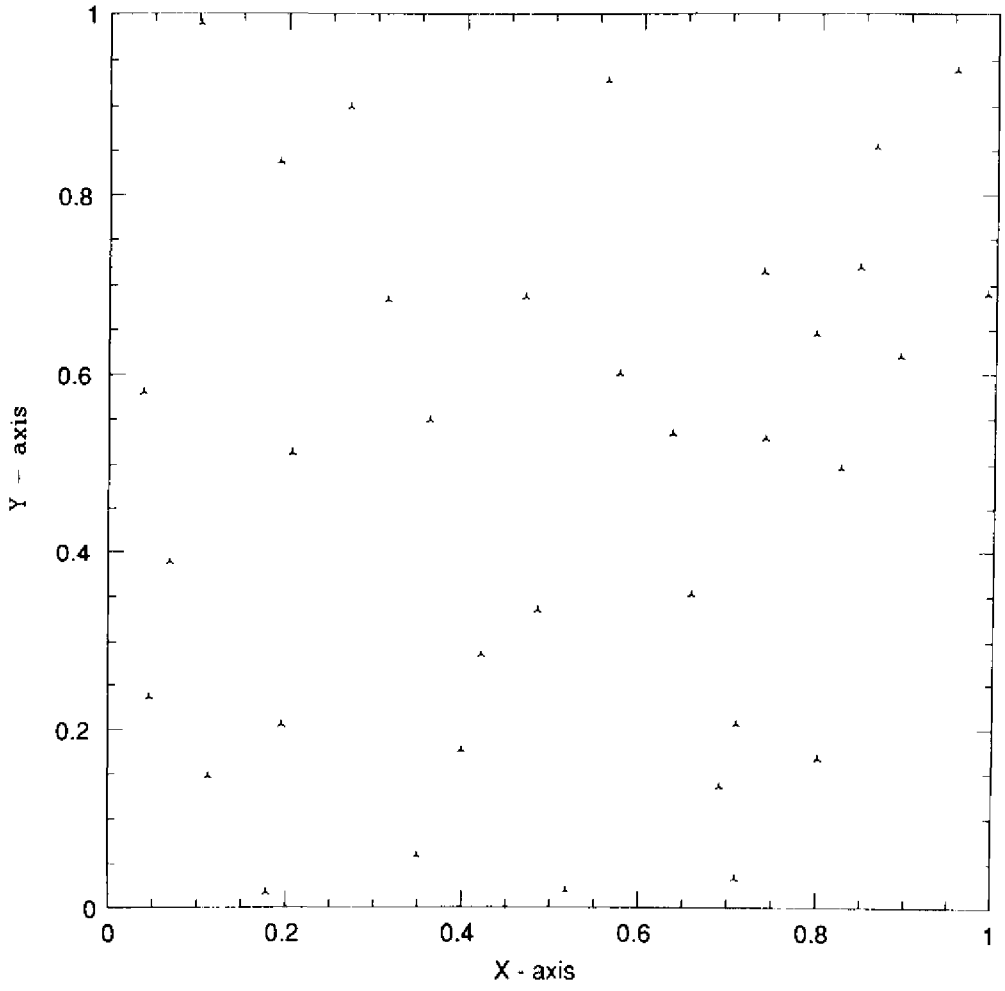
1
0.8
0.6
0.4
0.2
0
Y - axis
0
0.2
0.4
0.6
0.8
1
X - axis

Fig.7a

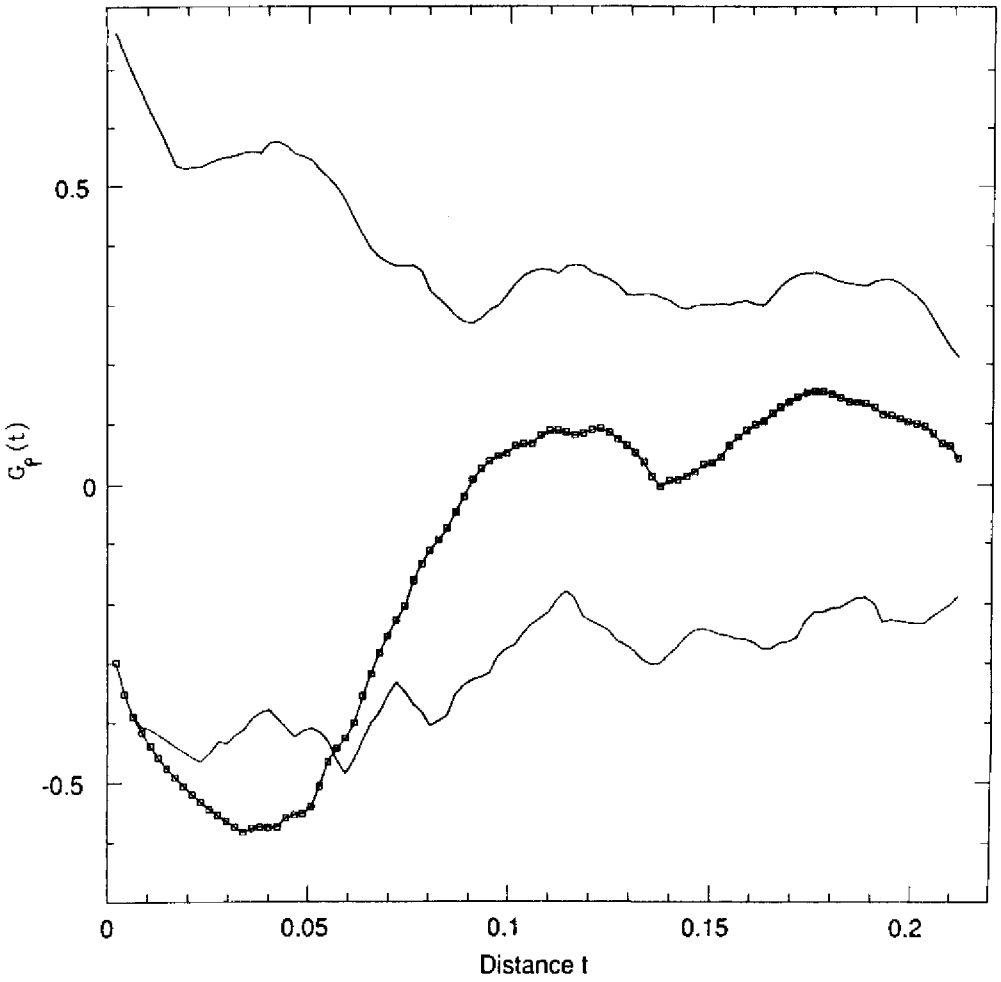
0.5
0
-0.5
$G_\rho(t)$
0
0.05
0.1
0.15
0.2
Distance t

Fig.7b